Science of the Total Environment 753 (2021) 141788

Contents lists available at ScienceDirect

Science of the Total Environment

journal homepage: www.elsevier.com/locate/scitotenv

Dry deposition of particulate matter and its associated soluble ions on five broadleaved species in Taichung, central Taiwan

Tzu-Hao Su [a], Chin-Sheng Lin [a], Jiunn-Cheng Lin [b], Chiung-Pin Liu [a,*]

[a] Department of Forestry, National Chung Hsing University, 145, Xingda Rd., South Dist., Taichung 40254, Taiwan
[b] Taiwan Forestry Research Institute, Taipei 100, Taiwan

HIGHLIGHTS

- A field experiment was performed to measure the dry deposition flux and velocity of particulate matter on leaf surfaces.
- A significant relationship was observed between the ambient concentration and the dry deposition flux of PM.
- The long-range transport of sulfate was observed during the winter monsoon.
- The experimental results were consistent with results obtained using the i-Tree model.

GRAPHICAL ABSTRACT

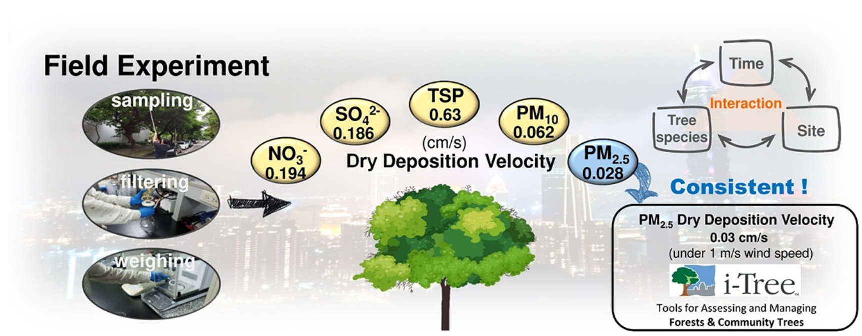

ARTICLE INFO

Article history:
Received 24 June 2020
Received in revised form 7 August 2020
Accepted 17 August 2020
Available online 21 August 2020

Editor: Elena Paoletti

Keywords:
Urban forest
Air pollution
Dry deposition velocity
Interception
$PM_{2.5}$
I-tree model

ABSTRACT

Many studies have estimated particulate matter (PM) removal by urban trees using dry deposition models; however, few studies have quantified the accuracy of their results. Thus, this study investigated the dry deposition of PM and its associated soluble ions in five broadleaved species in three districts of Taichung, central Taiwan, through field experiments. The total suspended particulate (TSP) dry deposition flux on leaf surfaces varied with sampling time, site, and tree species. By contrast, single-factor effects were observed for PM_{10} and $PM_{2.5}$. The average dry deposition velocities of TSPs, PM_{10}, and $PM_{2.5}$ were 0.63, 0.062, and 0.028 cm s^{-1}, respectively. Moreover, the dry deposition velocities of sulfate and nitrate were estimated to be 0.186 and 0.194 cm s^{-1}, respectively. A significant relationship was observed between the ambient concentration and the dry deposition flux for all size fractions of PM. By contrast, weak and negative correlations were found between particle deposition velocity and wind speed. The measured $PM_{2.5}$ dry deposition velocity was approximately equal to the dry deposition velocity obtained with the i-Tree model (0.03 cm s^{-1}), which indicated the promising application potential of i-Tree in Taiwan. Compound and rough leaves, such as leaves of the Taiwan golden-rain tree, intercepted a high amount of $PM_{2.5}$, whereas the pongam tree, which has thin leaves and wax surfaces, exhibited the lowest TSP interception. Species difference mostly occurred in the dry deposition flux of nitrate rather than sulfate; however, the interception of sulfate by trees revealed the possibility of the long-range transport of air pollutants. The results of this study elucidate the dry deposition of PM and its associated soluble ions in real-world situations.

1. Introduction

With air pollution becoming an increasingly serious problem, the adverse effects of atmospheric particulate matter (PM) on human

* Corresponding author.
E-mail address: cpliu@nchu.edu.tw (C.-P. Liu).

https://doi.org/10.1016/j.scitotenv.2020.141788
0048-9697/

health have attracted increasing research attention. PM is defined as particles with a diameter of less than 100 μm (i.e., total suspended particulates [TSPs]). PM is mainly monitored as PM_{10} (PM with a diameter smaller than 10 μm) and $PM_{2.5}$ (PM with a diameter smaller than 2.5 μm). Over the past two decades, increased research attention has focused on $PM_{2.5}$ because of its high persistence in the atmosphere. $PM_{2.5}$ can penetrate deep into the lungs and is a considerable threat to human health because it contains toxic heavy metals (Chen et al., 2015a; Li et al., 2014; Wang et al., 2018; Zheng et al., 2016) and polycyclic aromatic hydrocarbons (Bandowe et al., 2014; Kong et al., 2018; Mohammed et al., 2016; Sosa et al., 2017; Xie et al., 2017). Taiwan, which is located in southeast China, suffers from air pollution due to coal burning and industrial emissions in China during the winter monsoon (Lin et al., 2007; Chen et al., 2015b; Hsu et al., 2016). In addition, many cities with high population density in western Taiwan have air pollution levels above the World Health Organization limits during late autumn and early spring. Local pollutant emissions in Taiwan originate from heavy traffic, power plants, steel factories, and other industries (Ho et al., 2003; Chen et al., 2016).

Depending on rainfall events, PM is removed from the atmosphere through dry or wet deposition processes (Beckett et al., 1998). During days without rain, trees in urban forests can purify air by intercepting PM with their leaves and branches due to the large surface area of their leaves and branches. Thus, studies on PM dry deposition onto leaf surfaces are extremely important, which can help to verify the ability of air purification by different tree species. The dry deposition of PM is influenced by its chemical properties, its surface characteristics, and the meteorological conditions. Performing direct accurate measurements of the dry deposition velocity of PM is difficult due to its small size (Long et al., 2001; Litschke and Kuttler, 2008). Cai et al. (2017) reviewed more than 150 studies published between 1960 and 2016 and concluded that the average deposition flux of PM on leaves is 1.71 ± 0.05 g m^{-2} wk^{-1} (approximately 10.18 mg m^{-2} h^{-1}). PM was extracted from leaves by using the dry method (Chen et al., 2016; Liu et al., 2012; Prajapati and Tripathi, 2008) or wet method (Beckett et al., 2000a; Prusty et al., 2005; Wang et al., 2013; Xu et al., 2018). The dry method is easy and quick and involves manually brushing the leaf; however, this method cannot be used to distinguish different sizes of the deposited PM. By contrast, in the wet method, water is used to wash the leaf and quantify different size fractions of PM through filtration. Numerous studies have quantitatively analyzed the particles deposited onto leaves; however, few studies have examined deposition flux. Most relevant studies have collected leaf samples at given times to investigate PM deposition for different tree species (Beckett et al., 2000b; Dzierżanowski et al., 2011; Popek et al., 2013; Sæbø et al., 2012; Sgrigna et al., 2015; Song et al., 2015), canopy layers (Hofman et al., 2014), distances from the road (Freer-Smith et al., 1997; Mori et al., 2015; Sgrigna et al., 2015), and leaf layers (surface or wax) (Dzierżanowski et al., 2011; Mori et al., 2015; Popek et al., 2013; Sgrigna et al., 2015). Few studies have conducted field measurements to estimate the dry deposition velocity of PM on leaves. These studies relied on the long-term estimation of the deposition flux of PM and the representative ambient concentration data. Because the aforementioned information has rarely been obtained through field measurements, the estimation of PM interception by urban trees can mostly rely on a limited set of parameters in deposition models.

Improving air quality is one of several ecosystem services that trees provide. The i-Tree Eco dry deposition model (simply referred to as i-Tree), which has been developed by incorporating tree parameters, the dry deposition speed of PM, environmental conditions, and economic benefits, is widely used to evaluate the monetary benefits of ecosystem services, including PM interception by urban forests (Nowak et al., 2013). Many studies have investigated PM_{10} and $PM_{2.5}$ removal by urban trees and their economic benefits using i-Tree model (Bottalico et al., 2016; Nowak et al., 2013; Selmi et al., 2016; Tallis et al., 2011). The PM dry deposition velocities in i-Tree were obtained from studies that used NaCl or KNO_3 for particle exposure and observed the deposition flux on leaves under different wind speed conditions. However, the characteristics of simulated particles may be different from those of real atmospheric PM. Furthermore, the i-Tree model only includes the $PM_{2.5}$ dry deposition velocity data (obtained through wind tunnel experiments) of fewer than 20 tree species under different wind speeds (Hirabayashi et al., 2015). However, Taiwan has different climate zones, which results in considerable biodiversity. Thus, the results of i-Tree are insufficiently generalizable to other types of leaves, and the simulation results may differ from the ground reality.

This study aimed to determine the variability in the dry deposition flux and velocity of PM and its associated soluble ions for different tree species, sites, and months. We conducted a field experiment with five indigenous tree species common in Taiwan to understand the dry deposition of PM onto leaves in the real world. The obtained results were compared with the parameters in the i-Tree model. We also examined the correlations 1) between the dry deposition flux and the PM concentration and 2) between the dry deposition velocity and meteorological factors (such as the wind speed, relative humidity, and temperature). The field study investigated the following hypotheses: (1) the dry deposition flux of PM and its associated soluble ions on leaves varies according to the sampling time, site, and tree species; (2) the dry deposition velocities of PM_{10} and $PM_{2.5}$ in i-Tree are inapplicable in field situations; (3) the dry deposition flux of PM on leaves is positively correlated with the ambient concentration of PM; and (4) significant correlations exist between meteorological factors and the dry deposition velocity of PM.

2. Materials and methods

2.1. Study area and monitoring stations

This study was conducted in Taichung, a city located in the central part of Taiwan (24°6′N, 120°40′E). Taichung is the second most populous city in Taiwan. It has a population of approximately 2.81 million people and covers an area of 2214 km^2. The world's third largest thermal power plant is located in Taichung. This power plant is widely considered to be a major contributor to air pollution in Taichung. We selected the most densely populated area of Taichung as the study area. This area covers only 10% of Taichung but accounts for approximately 70% of its population (approximately 9000 people per km^2) (Fig. 1). Due to the high population density in Taichung, road traffic is also a major source of air pollutants. In the study area, we selected three sampling sites close to the air quality and TSP monitoring stations, which were, from north to south: Nantun, Dali, and Wufeng. The air quality monitoring stations automatically provide hourly data on the ambient concentration of PM_{10}, $PM_{2.5}$, and meteorological factors, such as the temperature, relative humidity, precipitation, and wind speed. TSP monitoring stations provide daily manual monitoring data regarding the ambient TSP concentration twice a month and regarding the nitrate and sulfate concentration once a season (Fig. 1).

2.2. Plant material and sampling

We selected five broadleaved indigenous tree species that are common in Taiwan: the chinaberry tree (*Melia azedarach*), the Taiwan golden-rain tree (*Koelreuteria elegans*), the camphor tree (*Cinnamomum camphora*), bishop wood (*Bischofia javanica*), and the pongam tree (*Millettia pinnata*). *M. azedarach* and *K. elegans* are semideciduous tree species with leaves that fall from December to February, whereas the other three tree species are evergreen species. Excluding *C. camphora*, which has single leaves, all the other aforementioned tree species have compound leaves. Three trees were used as a triplicate for each species (Fig. 1). For each replication, healthy leaves were picked out randomly from its tree at a height of 3–5 m. To better represent the PM interception of one tree, we collected 3–4

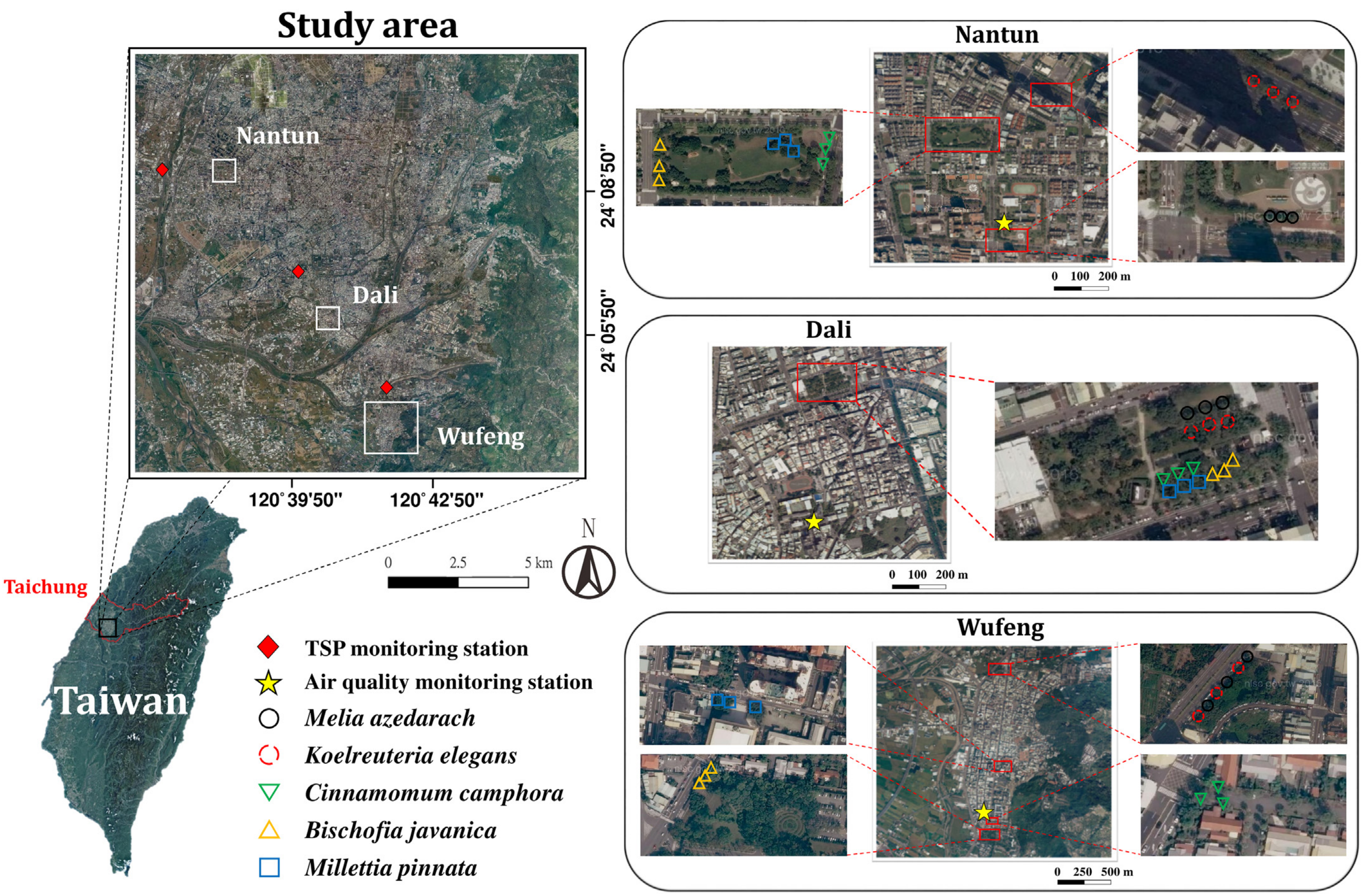

Fig. 1. Locations of the study sites, monitoring stations, and sampling trees in Taichung.

times the leaf area per sample collected in previous studies (Dzierżanowski et al., 2011; Sgrigna et al., 2015). The leaf area per sample ranged between 1000 and 1500 cm^2 in this study (approximately 20–30 leaflets of bishop wood and the pongam tree, 80–120 leaves of the camphor tree, and 150–220 leaflets of the chinaberry tree and Taiwan golden-rain tree). To represent monthly changes, leaf samples were collected on the following dates: September 26, October 31, and December 7, 2016, as well as January 6, February 1, March 5, March 31, May 1, May 29, June 29, July 26, and August 21, 2017. The sampling dates were adjusted due to rainfall events. Samples were collected almost once a month and represented 12 months of dry deposition from September 2016 to August 2017. In summary, 540 leaf samples were tested from three sampling sites, five tree species, three replicates, and 12 sampling times. Leaf samples were placed in plastic bags to avoid contamination, transported immediately to the laboratory, and stored at 4 °C until analysis.

2.3. Washing and filtering procedure

Particles were washed down from leaves using deionized water. Each leaf sample was placed into a 1.5-L plastic box, and 100 mL of deionized water was added to the box. After manually shaking the box for 5 min, the water was filtered into a beaker using a 100-μm stainless steel sieve to remove particles larger than 100 μm. Afterward, 1 mL of the filtered water was passed through a 0.45-μm syringe filter (hydrophilic polyethersulfone, No. 4485, Pall Corporation, East Hills, NY, USA) into a clean tube before further extraction. The filtered water was then subjected to ion analysis. The aforementioned washing and filtering procedure was repeated four times into the same beaker; however, the manual shaking time was adjusted to 15 s. The first washing procedure, which involved using only 100 mL of deionized water, aimed to avoid the effect of dilution. Therefore, a long manual shaking time was required in the first washing step to ensure that all of the soluble ions on the leaf surfaces were dissolved in water. Approximately 60%–70% of particles were washed out from the leaves into the beaker in the first step. Four additional washing steps were performed to remove all of the residual particles between the leaves. We conducted preliminary tests to confirm that more than 90% of different particle size fractions could be collected using the aforementioned method in the study area; however, if a large amount of PM is intercepted by tree leaves in other regions, additional washing procedures may be required. The final volume of filtered water that contained particles smaller than 100 μm was almost 500 mL. The aforementioned water was filtered again by using a 47-mm magnetic filter funnel (No. 4242, Pall Corporation, East Hills, NY, USA) connected to a vacuum pump (V-500, Büchi Labortechnik AG, Flawil, Switzerland) and passed through three preweighed filters, namely a nylon filter (pores: 10 μm; Startech, Changhua County, Taiwan), cellulose filter (pores: 2.5 μm; type 42, Whatman Corporation, Piscataway, NJ, USA), and mixed cellulose ester filter (pores: 0.45 μm; GN-6, Pall Corporation, East Hills, NY, USA). The aforementioned preweighed filters were first filtered using deionized water, dried at 60 °C for 1 h, and then weighed. The aforementioned procedure was performed several times to obtain stable filters and their preweighed values for further PM filtration. Changes in relative humidity affect weighing accuracy; therefore, the laboratory humidity was stabilized (35%–40%) to minimize the effect of humidity on the weighing process. In the PM filtration stage, a few filters were filtered only through deionized water as blanks to ensure the stability of the environment. After the PM filtration procedure, three types of filters were dried under the aforementioned condition and reweighed. Thus, three particle size fractions on the filters were collected. The deposition amounts of TSPs, PM_{10}, and $PM_{2.5}$ on the leaves could be estimated by subtracting the preweight from the postweight. Specifically, in this study, TSP, PM_{10}, and $PM_{2.5}$ are defined as particles with diameters of 0.45–100, 0.45–10, and 0.45–2.5 μm, respectively. All the filters were weighed in a microbalance with a precision of ±0.01 mg (AP125WD, Shimadzu Corporation, Kyoto, Japan) under stable ambient humidity. Subsequently, a static eliminator (QUICK440A, Farnell Corporation, London, UK) was used to avoid disturbance. In our sampling period, TSPs and their associated ions were continually measured, whereas PM_{10} and $PM_{2.5}$ were only measured during the last two deposition months (July and August 2017).

2.4. Analysis of soluble ions

The prepared water samples were analyzed through ion chromatography (IC; DX-120, Dionex, Sunnyvale, CA, USA) for nitrate (NO_3^-) and sulfate (SO_4^{2-}) ions. The IC apparatus comprised a column (AS9-HC, Dionex), guard column (AG-24A, Dionex), suppressor (ASRS-300, Dionex), conductivity detector, and gradient pump. An eluent (9 mM Na_2CO_3) was used for anion detection. The limits of detection were less than 0.1 mg L^{-1}, and the detection method was linear ($R^2 > 0.999$) for both NO_3^- and SO_4^{2-} detection with standard reference materials (Merck, Darmstadt, Germany).

2.5. Monitoring data from stations

The air pollutant monitoring data and meteorological conditions obtained from both types of monitoring stations in the dry deposition periods are summarized in Table S1. According to Fang et al. (2003), PM_{10} contributes more than 50% of the mass of TSPs; thus, a strong relationship exists between PM_{10} and TSPs. Because the monitoring periods of TSPs in this study were not widely distributed and the TSP monitoring stations were further away from the sampled trees than the PM_{10} monitoring stations were, we converted the hourly PM_{10} monitoring data into TSP data instead of using TSP monitoring data directly. We analyzed the TSP and PM_{10} monitoring data of the past 3 years for each site, and good linear correlations were observed between the TSP and PM_{10} monitoring data ($R^2 > 0.70$ for the three sites). Thus, linear regression could be performed to convert the hourly PM_{10} monitoring data into hourly TSP data. The average concentrations of TSPs, the associated sulfate, and the associated nitrate for all the sites during the sampling period were 59.18, 4.00, and 3.79 μg m^{-3}, respectively. The average concentrations of PM_{10} and $PM_{2.5}$ at the three selected sites during the analysis period (July and August) were 31.05 and 14.69 μg m^{-3}, respectively. The PM and ion concentration data from each monitoring station were used to calculate the dry deposition velocities. Moreover, meteorological data were used to determine the relationships of the wind speed, relative humidity, and temperature with the dry deposition velocities of PM.

2.6. Estimation of dry deposition velocity

The dry deposition velocity of PM and its associated ions on leaves is estimated using Eq. (1).

$$F = V_d \times C \tag{1}$$

where F is the dry deposition flux of PM (μg cm^{-2} s^{-1}), V_d is the dry deposition velocity of PM (cm s^{-1}), and C is the ambient concentration of PM (μg cm^{-3}).

After the washing and filtering procedure, the amount of PM intercepted by tree leaves was quantified. To estimate the dry deposition flux of PM and its associated ions on leaves, information regarding the deposition area and deposition time was required. The leaf area was obtained from scanned images of leaves by using ImageJ software (National Institutes of Health, Bethesda, MD, USA). Furthermore, the dry deposition period was confirmed using the hourly rainfall data obtained from the air quality monitoring stations. The precipitation threshold at which all particles were considered to be washed out from the leaves was assumed to be the product of 0.2 (mm) and the leaf area index (LAI) of the sampled trees. This threshold was obtained with reference to previous studies that have indicated that the water storage capacity is 0.2 mm per unit leaf area (Nowak et al., 2013; Wang et al., 2008). The threshold was also used in i-Tree model. In general, the LAI of street trees does not exceed 5 (Armson et al., 2013; Gonzalez-Sosa et al., 2017). The canopy of all the different species of sampled trees was not particularly dense. Thus, if the precipitation in the study area was higher than 1 mm (the product of 0.2 and 5), then the dry deposition of PM would be completed and new dry deposition would begin after the end of the precipitation. In this study, the dry deposition period in the sampling months ranged from 83 h (April 2017, Nantun) to 437 h (January 2017, Dali). The dry deposition flux could be calculated using all of the aforementioned information. The dry deposition velocity of PM and its associated soluble ions could be determined by dividing the dry deposition flux by the mean ambient concentration data obtained from the monitoring stations.

2.7. Statistical analysis

To test whether the dry deposition flux and velocity of PM and its associated soluble ions varied among tree species, study sites, and sampling times, a three-way analysis of variance (ANOVA) with replication (5 species × 3 sites × 12 times) was performed, followed by an application of the Holm–Sidak method. In Fisher's least significant difference (LSD) test, the type I error rate (α) increases with increasing pairwise comparisons. Therefore, the Holm–Sidak method is superior to Fisher's LSD test for reducing the α error. Furthermore, the Holm–Sidak method is less conservative than other post hoc methods, such as the Bonferroni test. The raw flux and velocity data were converted to a logarithmic scale because the log-normal data were normally distributed. Spearman' correlation analysis was used to evaluate the relationships between 1) dry deposition fluxes and concentrations and between 2) dry deposition velocities and meteorological factors. The Spearman correlation coefficient is denoted by "rho" in this study. All statistical analyses were performed using SPSS version 20 (IBM Corporation, Amonk, NY, USA; released 2011) and SigmaPlot 13.0 (Systat Software Inc., San Jose, CA, USA).

3. Results

3.1. Dry deposition flux

3.1.1. TSPs

The significant effects were observed for all single- and multiple-factor interactions among the sampling time, site, and species for TSP flux (Fig. 2A). At Nantun, *C. camphora* and *B. javanica* had a significantly higher TSP dry deposition flux ($p < 0.001$ and $p < 0.05$, respectively) than the other tree species did. At Dali, *K. elegans* had a significantly higher TSP dry deposition flux ($p < 0.05$) than *B. javanica* and *M. azedarach* did. At Wufeng, *B. javanica* and *K. elegans* exhibited a higher TSP dry deposition flux than the other species did. Considerable differences in the TSP dry deposition flux were observed among the tree species at Wufeng than at the other two sites. Moreover, the TSP dry deposition fluxes for *C. camphora* and *M. azedarach* were higher than that for *M. pinnata* ($p < 0.001$ for all differences at Wufeng) (Fig. 2B). During most months of the sampling period, the TSP dry deposition flux was higher at Wufeng than at the other sites and was lower for *M. pinnata* than for the other tree species. The major peak for TSPs occurred in February 2017 for most of the sites and species. Significant differences were observed among the tree species in each month except June and

A

Dry deposition flux								
TSP			NO_3^-			SO_4^{2-}		
Parameter	*p* value		Parameter	*p* value		Parameter	*p* value	
time	<0.001	***	time	<0.001	***	time	<0.001	***
site	<0.001	***	site	<0.001	***	site	<0.001	***
species	<0.001	***	species	<0.001	***	species	<0.001	***
time x site	<0.001	***	time x site	0.011	*	time x site	<0.001	***
time x species	<0.001	***	time x species	0.041	*	time x species	<0.001	***
site x species	<0.001	***	site x species	<0.001	***	site x species	<0.001	***
time x site x species	<0.001	***	time x site x species	<0.001	***	time x site x species	0.365	ns

B

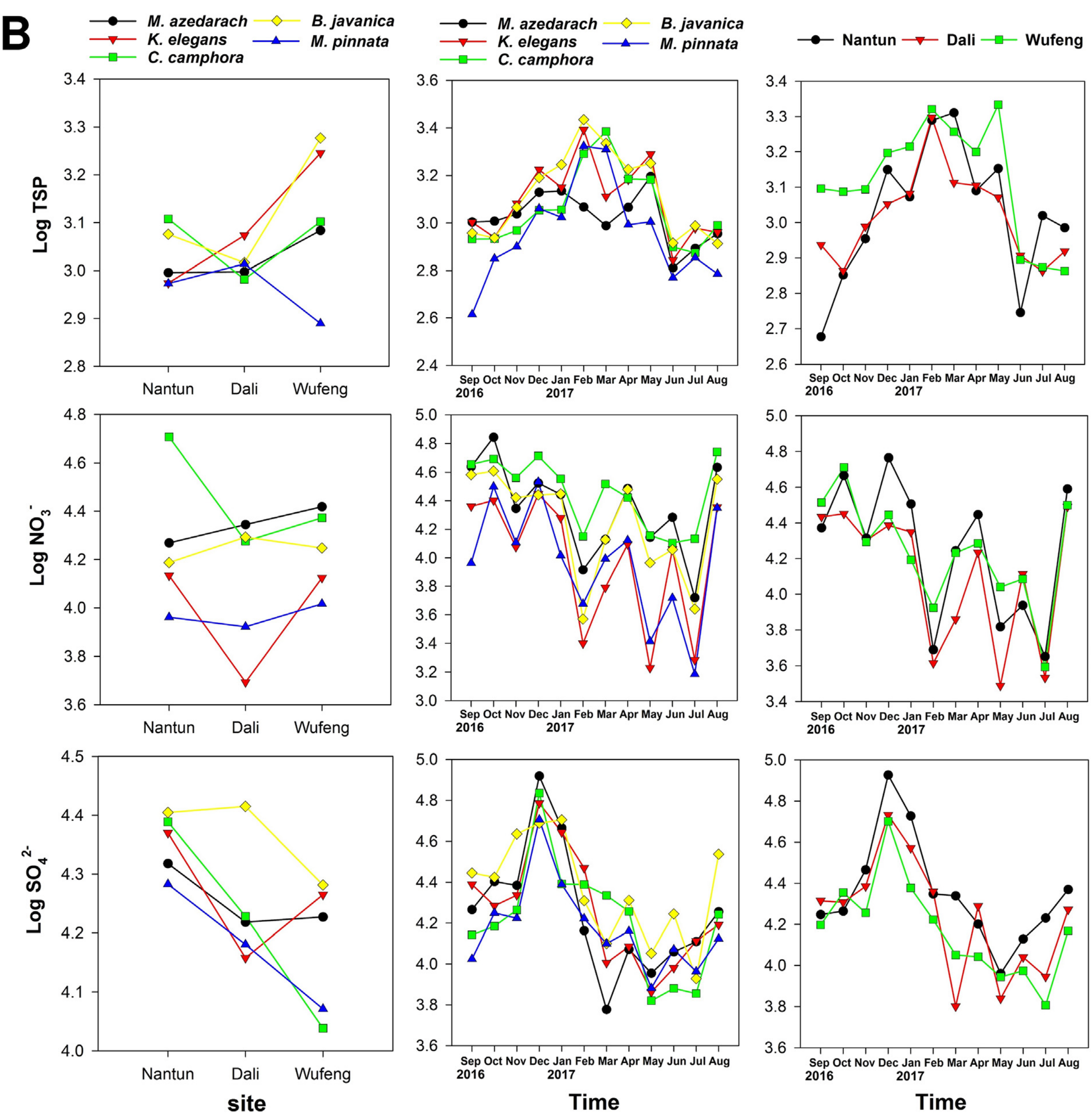

Fig. 2. Three-way ANOVA of the dry deposition fluxes of TSPs, NO_3^-, and SO_4^{2-} on leaves: (A) summary table of the statistics and (B) plots for the significant two-way interaction effects (note: source data of TSPs [$\mu g\ m^{-2}\ h^{-1}$] and their associated ions [$ng\ m^{-2}\ h^{-1}$]; ***, significant at the 0.001 level; **, significant at the 0.01 level; *, significant at the 0.05 level; and ns, not significant).

July 2017 (Fig. 2B). The average TSP dry deposition flux for all the sampling sites, species, and times was 1.31 mg m^{-2} h^{-1}.

3.1.2. Nitrate and sulfate

Except for the three-factor interaction for sulfate, significant effects were observed for all single- and multiple-factor interactions among the sampling time, site, and species for nitrate and sulfate fluxes (Fig. 2A). The nitrate depositions on *K. elegans* and *M. pinnata* were significantly lower than those on the other tree species at all the sites; however, the sulfate depositions on *C. camphora* and *M. pinnata* were significantly lower than those on the other tree species only at Wufeng. A significant higher sulfate deposition was noted on *B. javanica* at Dali (Fig. 2B). During the sampling period, significant species differences were noted in the dry deposition flux of nitrate in most of the sampling months (except February, April, and December). The nitrate deposition on *C. camphora* was usually high, and those on *K. elegans* and *M. pinnata* were usually low. In contrast, no significant differences in sulfate deposition were observed among the tree species from December to April (including March due to the greater variance); however, the sulfate deposition on *B. javanica* was mostly higher, and those on *C. camphora* and *M. pinnata* were mostly lower during the other months. Moreover, the nitrate flux at the three sites generally exhibited no difference over the sampling months. By contrast, the sulfate flux at Nantun was higher than that at the other two sites over half the sampling period. Furthermore, the results indicated different monthly trends of dry deposition flux for nitrate and sulfate. The major peak for sulfate occurred in December 2016 for different sites and species, whereas the dry deposition flux of nitrate fluctuated from winter to summer (Fig. 2B). The average nitrate and sulfate dry deposition fluxes for all the sampling sites, species, and times were 0.025 and 0.028 mg m^{-2} h^{-1}, respectively.

3.1.3. PM_{10} and $PM_{2.5}$

The results of the dry deposition flux indicated the absences of two- and three-way interaction effects among the sampling times, sites, and species for PM_{10} and $PM_{2.5}$ (Fig. 3A). The dry deposition fluxes of PM_{10} and $PM_{2.5}$ were higher in July than in August ($p < 0.001$). The PM_{10} fluxes at Nantun and Dali were significantly higher than that at Wufeng ($p < 0.05$). Moreover, the $PM_{2.5}$ flux exhibited significant differences among the sampled tree species. The $PM_{2.5}$ flux for *K. elegans* was significantly higher than that for *C. camphora* ($p < 0.01$) (Fig. 3B). The average PM_{10} and $PM_{2.5}$ dry deposition fluxes for all the sampling sites, species, and times were 0.070 and 0.015 mg m^{-2} h^{-1}, respectively.

3.2. Dry deposition velocity

The dry deposition velocity of different particle sizes was calculated using concentration monitoring data, and the same concentration value was applied for all tree species at each site and time. Therefore, the differences in the dry deposition velocities of different species were the same as the differences in the dry deposition fluxes in Fig. 2. The interaction between time and site was significant only for TSPs (Fig. 4A), and the dry deposition velocity of the TSPs was significantly higher at Wufeng than at the other sites in most of the sampling months. The dry deposition velocity of PM_{10} was higher at Nantun than at Wufeng ($p = 0.025$). Furthermore, the dry deposition velocities of PM_{10} and $PM_{2.5}$ were higher in July than in August ($p = 0.011$) (Fig. 4B). The average dry deposition velocities of TSPs, PM_{10}, and $PM_{2.5}$ for all the sites, species, and times were estimated to be 0.63, 0.062, and 0.028 cm s^{-1}, respectively. We also calculated the dry deposition velocity of ions from Eq. (1) by using the mean of the seasonal concentration data obtained from TSP monitoring stations. The average dry deposition velocities of nitrate and sulfate were 0.194 and 0.186 cm s^{-1}, respectively.

3.3. Leaf particle loading trend

We evaluated the dry deposition of PM on leaves at different times by dividing the dry deposition amount at each time segment (μg m^{-2}) by the ambient concentration (μg m^{-3}). This ratio is equal to the product of the dry deposition velocity (m h^{-1}) and dry deposition time (h). This calculated value, namely the dry deposition distance, can exclude the influence of different PM concentrations in each deposition period and indicate the variation in the dry deposition of PM on leaves over different deposition times. The average dry deposition distance of TSPs increased with an increase in the deposition time for the average results of all the tree species. No abnormal values were observed under different rainfall intensities. The fitted regression model between the dry deposition distance and the deposition period among all the tree species was linear ($y = 27.286x – 992.277$; $R^2 = 0.656$, $p < 0.001$) (Fig. 5).

3.4. Correlation analysis

3.4.1. Relationship between dry deposition fluxes and ambient concentrations

The results indicated that the dry deposition flux was significantly correlated with the ambient concentration for all particle sizes. TSPs exhibited a stronger and more significant correlation between the flux and the ambient concentration (rho = 0.374, $p < 0.001$) than PM_{10} and $PM_{2.5}$ did. PM_{10} and $PM_{2.5}$ exhibited weak but significant correlations between the flux and the ambient concentration (rho = 0.269 [$p = 0.005$] and 0.209 [$p = 0.024$], respectively) (Fig. 6).

3.4.2. Relationship between dry deposition velocity and meteorological factors

The dry deposition velocity of TSPs was negatively correlated with temperature, relatively humidity, and wind speed; however, significant results were obtained only for temperature and relative humidity (rho = −0.194 [$p < 0.001$] and − 0.116 [$p < 0.01$], respectively). By contrast, the dry deposition velocities of PM_{10} and $PM_{2.5}$ had a significantly positive correlation with relative humidity (rho = 0.286 [$p < 0.01$] and 0.336 [$p < 0.01$], respectively) but a significantly negative correlation with wind speed (rho = −0.189 [$p < 0.05$] and − 0.324 [$p < 0.01$], respectively) (Table 1).

4. Discussion

4.1. Spatial and temporal variations in the dry deposition flux of PM

The significant three-way interaction effect for TSPs revealed that the tree species had different PM interception abilities at different sites and times (Fig. 2A). For example, *M. azedarach* had higher PM interception abilities than *M. pinnata* at all sampling times except for February and March. Moreover, *M. azedarach* had a significantly higher PM interception ability than *M. pinnata* only at Wufeng (Fig. 2B). This phenomenon could be attributable to the difference in the same species among different sites and times. The leaves of *M. azedarach* began to fall in January and regrow after April, and less defoliation occurred at Wufeng than that at the other sites. Differences in tree architectures and aerodynamic characteristics may lead to different PM interception levels by leaves (Beckett et al., 2000a), and a sparse canopy may adversely affect PM interception. Furthermore, the difference of microclimatic conditions among these sites could also influenced the PM interception by different species. Thus, complicated results may be obtained, and estimations at different sites and times may be required when determining the ability of different tree species to intercept TSPs in field situations. In addition, all the interaction effects exhibited nonsignificant results for PM_{10} and $PM_{2.5}$ (Fig. 3A), which indicated that the deposition results of these PM were less variable than those of TSPs. The PM_{10} and $PM_{2.5}$ deposition fluxes were higher in July than in August (Fig. 3B). This result was observed for different sites and

A

Dry deposition flux					
PM_{10}			$PM_{2.5}$		
Parameter	***p* value**		**Parameter**	***p* value**	
time	<0.001	***	time	<0.001	***
site	0.045	*	site	0.697	ns
species	0.765	ns	species	0.008	**
time x site	0.995	ns	time x site	0.064	ns
time x species	0.999	ns	time x species	0.718	ns
site x species	0.654	ns	site x species	0.411	ns
time x site x species	0.968	ns	time x site x species	0.227	ns

B

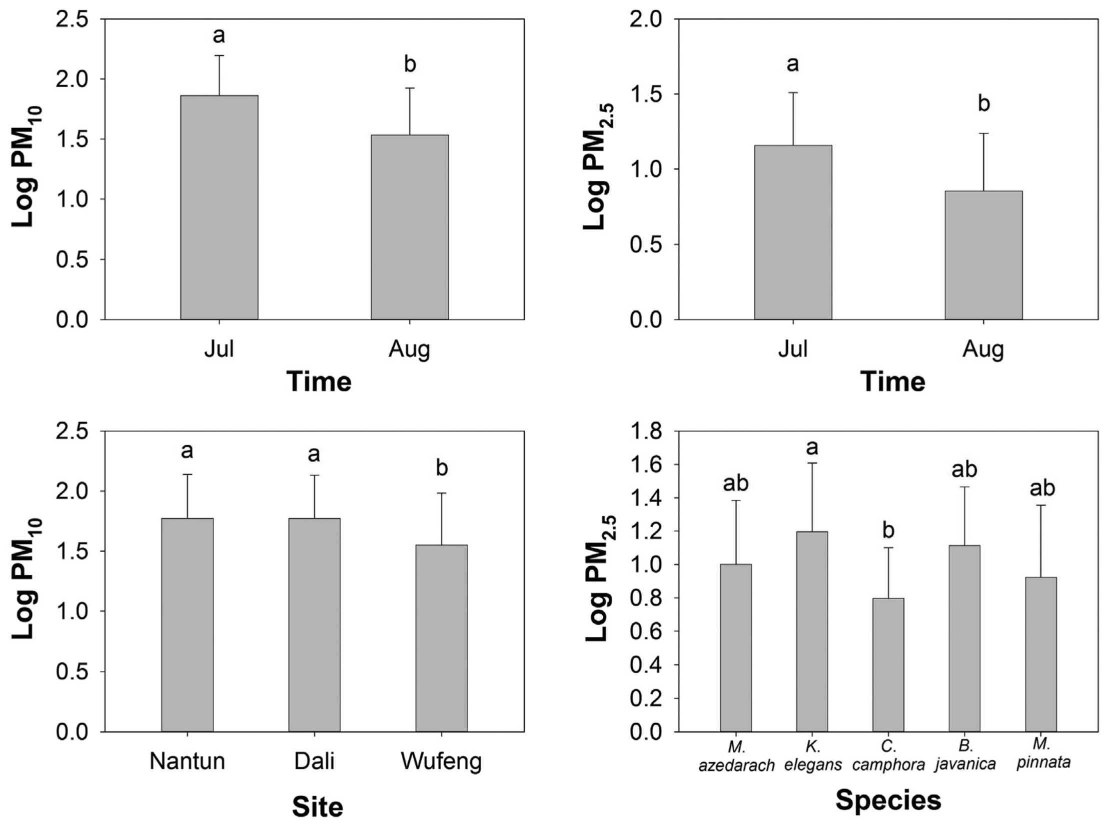

Fig. 3. Three-way ANOVA of the dry deposition fluxes of PM_{10} and $PM_{2.5}$ on leaves: (A) summary table of the statistics and (B) plots for the significant main effects (note: source data of PM_{10} and $PM_{2.5}$ [μg m^{-2} h^{-1}]; *** significant at the 0.001 level; ** significant at the 0.01 level; * significant at the 0.05 level; ns, not significant; and thin vertical bars represent standard deviation).

tree species (no multiple-factor interactions). Thus, a high PM pollution based on a large amount of PM interception was observed in July for all the tree species, as indicated in Table S1. The obtained results have applications in the environmental monitoring of PM by using street trees as bioaccumulators. Furthermore, the TSP dry deposition flux on leaves for different sites and species was higher from winter to early spring than during the other months of the sampling period (Fig. 2B). The period from winter to early spring was also the air pollution season in Taichung. Poor vertical mixing and pollutant dispersion as well as low wind speed and rainfall occurred during this period, which resulted in an increase in PM concentration (Yang, 2002).

Unlike the deposition of small particles (PM_{10} and finer particles), TSP deposition on street trees may be easily affected by fugitive road dust; thus, the long-term determination of TSP deposition for multiple experimental sites is essential. In, addition, epicuticular wax on leaves aids the capture of small particles (Weerakkody et al., 2018) but not large particles (i.e., dust) (Liu et al., 2012). The same results were obtained for *M. pinnata*, which has thin leaves and a waxy surface. *M. pinnata* exhibited the lowest TSP interception among the tree species. Except for *M. pinnata*, most of the tree species exhibited close TSP deposition fluxes at different sampling times (Fig. 2B). This finding agrees with that of Xu et al. (2018), who tested the PM deposition on leaves for 17 plant species in Beijing, China. Most of the broadleaved species in Xu et al. (2018) exhibited similar levels of TSP interception. Moreover, we selected the months of July and August for the analysis to avoid the influence of defoliation on PM_{10} and $PM_{2.5}$ depositions. No significant differences in PM_{10} deposition were observed among the species; however, a significantly higher $PM_{2.5}$ deposition was

A

Dry deposition velocity								
TSP			**PM10**			**PM2.5**		
Parameter	***p* value**		**Parameter**	***p* value**		**Parameter**	***p* value**	
time	<0.001	***	time	0.011	*	time	0.011	*
site	<0.001	***	site	0.025	*	site	0.232	ns
time x site	<0.001	***	time x site	0.967	ns	time x site	0.109	ns

B

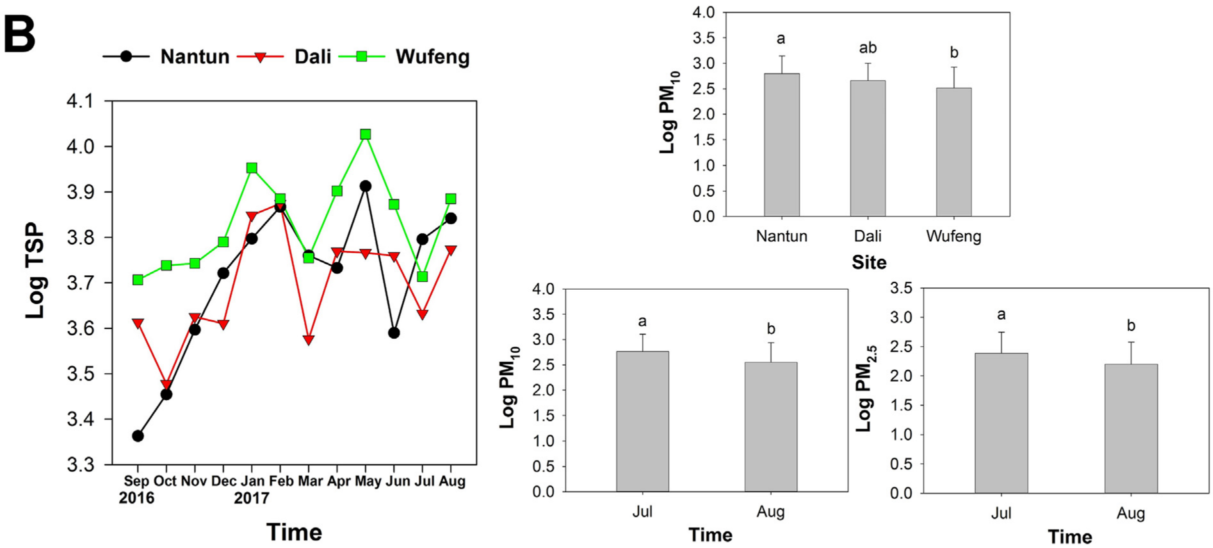

Fig. 4. Three-way ANOVA of the dry deposition velocity of TSPs, PM_{10}, and $PM_{2.5}$ on leaves: (A) summary table of the statistics and (B) plots for significant two-way interaction effects on TSPs and the main effects on PM_{10} and $PM_{2.5}$ (note: source data of TSPs, PM_{10}, and $PM_{2.5}$ [$\mu m\ s^{-1}$]; ***, significant at the 0.001 level; **, significant at the 0.01 level; *, significant at the 0.05 level; ns, not significant; and thin vertical bars represent standard deviation).

observed for *K. elegans* than for *C. camphora* (Fig. 3B). This finding agrees with that of Chen et al. (2017), who reported that the differences in PM interception among tree species mostly occur with respect to small particles due to the variation in leaf microstructures. Studies have indicated that hairy leaves can accumulate a higher amount of PM than smooth leaves can (Leonard et al., 2016; Sæbø et al., 2012). The leaves of *K. elegans*, which were pinnately compound leaves with rough surfaces, could intercept a relatively high amount of $PM_{2.5}$. By contrast, the leaves of *C. camphora* were smooth and hairless. Moreover, the petiole of *C. camphora* was longer than that of the other species. Consequently, *C. camphora* was shaken easily by winds, which may cause the resuspension of PM.

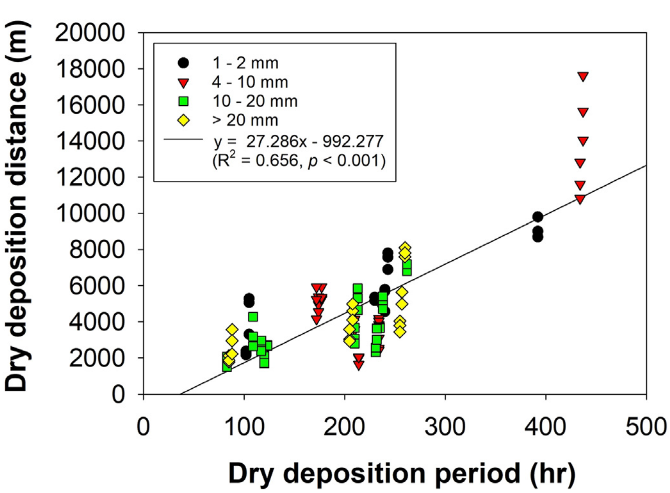

Fig. 5. Linear relationship between the dry deposition distance of TSPs and the dry deposition period (note: each dot represents the mean value of five tree species; different colors represent different precipitation levels before the beginning of dry deposition; [$n = 108$]).

The average TSP deposition flux from this study (1.31 $mg\ m^{-2}\ h^{-1}$) was approximately 7.8 times lower than the integrated result in Cai et al. (2017). This discrepancy was due to most of the data in Cai et al. (2017) being obtained from countries with high air pollution, such as China and India (e.g., Liu et al., 2012; Prusty et al., 2005; Wang et al., 2013). Another reason for the aforementioned discrepancy is that the type of deposited PM was unclear in the study of Cai et al. Without undergoing an initial filtration through a 100 μm sieve, the particles deposited on leaves were often classified as "dust" rather than suspended PM (e.g., Prajapati and Tripathi, 2008; Wang et al., 2013). The inclusion of particles larger than 100 μm, which originate from plant debris, leaf hair, or soil dust, will result in the overestimation of the dry deposition of PM. Our TSP deposition results were similar to those of studies conducted in countries with relatively low air pollution (e.g., Beckett et al., 2000a) or close particle size fractions (e.g., Xu et al., 2018). However, our PM_{10} and $PM_{2.5}$ results (with the averages of 0.070 and 0.015 $mg\ m^{-2}\ h^{-1}$, respectively) were considerably lower than those of other studies. For example, the PM_{10} and $PM_{2.5}$ deposition amounts estimated in this study were approximately 5 and 12 times lower than those estimated by Chen et al. (2016), respectively, and approximately 140 and 640 times lower than those estimated by Xu et al. (2018), respectively. This phenomenon was primarily explained by the relatively low PM concentration in our study area.

4.2. Spatial and temporal variations in the dry deposition flux of soluble ions

Significant two- or three-factor interactions were found for nitrate, whereas only two-factor interactions were found for sulfate (Fig. 2A).

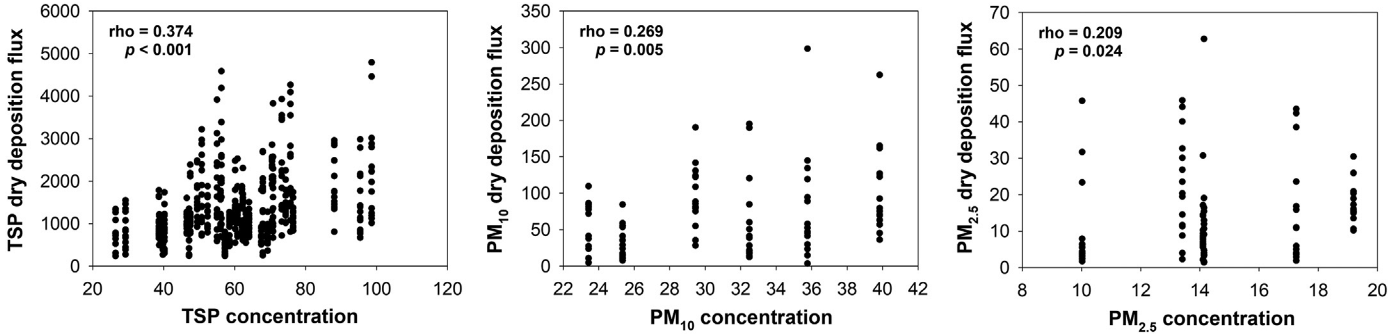

Fig. 6. Spearman correlation between the dry deposition flux and the ambient concentration for TSPs ($n = 540$), PM_{10} ($n = 90$), and $PM_{2.5}$ ($n = 90$) (note: flux [μg m^{-2} h^{-1}]; concentration [μg m^{-3}]).

These findings indicate that the results for sulfate were more consistent than were those for nitrate. For example, the changes in sulfate deposition at each sampling site differed depending on the time (Fig. 2B); however, the same changes were observed in the sulfate deposition results for all the tree species (significant for site and time). This finding indicates that all the species effectively intercepted particulate sulfate, and these species can be used as tools to monitor monthly air quality at different sites. Moreover, the amount of sulfate deposition on *B. javanica* was significantly higher than that on most of the other species in all the sampling months except for the period between December 2016 and April 2017. This result was observed at all the sampling sites (significant for species and time; Fig. 2B). Moreover, the amount of sulfate deposition on *B. javanica* was significantly greater than that on most of the other species at different sites, particularly at Dali. This result was observed throughout the sampling period (significant for species and site). The aforementioned results indicate that *B. javanica* is an effective species for intercepting particulate sulfate. *K. elegans* and *M. pinnata* exhibited lower amounts of particulate nitrate deposition than the other species at different sites and times, which suggests that *K. elegans* and *M. pinnata* do not effectively intercept particulate nitrate (Fig. 2B).

A major peak was observed in the dry deposition flux of sulfate for different sites and species in December, which was earlier than the peak of the TSP flux (February and March) (Fig. 2B). This result indicated that the composition of TSPs varied considerably. Sulfate and nitrate are considered derivatives of gaseous pollutants (SO_2 and NO_x) and major components of PM, particularly fine PM ($PM_{2.5}$) (Horváth, 2003; Tsai et al., 2012). However, the concentration of SO_2 was not particularly high at the three selected sites over the entire study period; thus, the increasing sulfate concentration possibly originated from direct emissions. Coal burning contributed a larger amount of sulfate than did nitrate (Ma et al., 2017). Moreover, the burning of large amounts of coal for heat in China increases sulfate emissions, which may be transported to Taiwan through the winter monsoon. This finding agrees with that of Chang et al. (2000), who found that most of the sulfate dry deposition associated with long-range transport occurred during the northeasterly monsoon (from December to January). The dry deposition flux of nitrate had several peaks in this study (Fig. 2B). Moreover, the atmospheric nitrate was attributed to vehicle emissions (Han et al., 2007), which suggested that the nitrate flux was mostly related to the local traffic. Compared with the results for sulfate deposition, the trees species exhibited greater variations in the nitrate deposition (Fig. 2B). This phenomenon could be related to the different emission types of sulfate, which originates from industrial emissions deposited from the upper atmosphere. By contrast, nitrate deposition originates from road emissions and thus can be easily influenced by different traffic or microclimatic conditions.

4.3. Dry deposition velocity of PM and ions

Wufeng exhibited a significantly higher TSP deposition velocity (Fig. 4B) and deposition flux (Fig. 2B) than the other sites during most months of the sampling period, which indicated that the relatively higher TSP flux at Wufeng was caused by the quickly deposition of particles. The TSP deposition velocity exhibited the same variation pattern at the three sites throughout the year (Fig. 4B); thus, the monthly changes in the meteorological conditions of the entire study area probably contributed to the differences in the results for different months. Chen et al. (2012) found that the dry deposition velocity of TSPs in the urban forest landscape was 1.44 cm s^{-1} in Guangzhou, China. This value is approximately 2.3-times larger than our result. The average wind speed in the aforementioned location (1 m s^{-1}) was similar to that in the study area; however, Chen et al. and this study used different methods to measure TSP deposition. Compared with deposition collecting plates made from polyvinyl chloride (PVC), tree leaves swing more freely and even turn upside down, which may lead to strong particle resuspension. To accurately understand PM purification by leaf interception, leaf collection and PM extraction are essential. We collected deposited TSPs from different types of leaves in three districts over a period of 1 year to determine the real deposition velocity. The average TSP deposition velocity was estimated to be 0.63 cm s^{-1}. Because the TSP dry deposition velocity was mainly influenced by gravity, the TSP dry deposition velocity was more stable than the $PM_{2.5}$ dry deposition velocity. Thus, the TSP dry deposition velocity is valuable

Table 1
Spearman correlation analysis results for the calculated dry deposition velocity of PM and meteorological factors.

	Temp.	RH	WS	TSP V_d		Temp.	RH	WS	PM_{10} V_d	$PM_{2.5}$ V_d
Temp.	1				Temp.	1				
RH	**0.125****	1			RH	**0.600*****	1			
WS	**0.583*****	−0.028	1		WS	−0.086	**−0.714*****	1		
TSP V_d	**−0.194*****	**−0.116****	−0.033	1	PM_{10} V_d	0.025	**0.286****	**−0.189***	1	
					$PM_{2.5}$ V_d	0.170	**0.336****	**−0.324****	**0.412*****	1

(Note: Temp., temperature; RH, relative humidity; WS, wind speed; TSP, total suspended particulate; V_d, dry deposition velocity; *, significant at the 0.05 level; **, significant at the 0.01 level; and ***, significant at the 0.001 level.)

for calculating the TSP interception by a large urban forest area by using concentration monitoring data.

The variations in the dry deposition velocities of PM_{10} and $PM_{2.5}$ at different sites and times exhibited similar patterns to the variations in the results for the deposition flux (Figs. 3B and 4B). This finding indicated that the PM concentrations were similar at different sites and times [according to Eq. (1)]. Thus, the changes in deposition velocity influenced the deposition flux. However, the mean PM_{10} dry deposition velocity is used as a fixed parameter in i-Tree, meaning that all spatial and temporal differences of dry deposition flux could be explained by the monitored ambient concentrations. The average dry deposition velocity of PM_{10} in i-Tree is 0.64 cm s^{-1} (Lovett, 1994), which is close to our average TSP deposition but more than 10 times larger than our average PM_{10} deposition (0.062 cm s^{-1}). This finding reveals that i-Tree overestimates the PM_{10} interception by urban forests. Moreover, this finding verifies hypothesis 2. The average $PM_{2.5}$ dry deposition velocity in i-Tree is 0.03 cm s^{-1} (under a wind speed of 1 m s^{-1}; Hirabayashi et al., 2015). This value is surprisingly consistent with the average $PM_{2.5}$ dry deposition velocity obtained in this study (0.028 cm s^{-1}). This finding suggests that i-Tree can be used for determining the $PM_{2.5}$ interception by tree leaves at the scale of the study area. However, the water-soluble components of $PM_{2.5}$ may be reduced by the washing and filtering procedure. Thus, the similar $PM_{2.5}$ dry deposition values in i-Tree and the present study mainly refer to the insoluble components of $PM_{2.5}$. Furthermore, the estimated dry deposition velocities of nitrate and sulfate were similar in this study (0.194 and 0.186 cm s^{-1}, respectively). Because of the limitations of our washing method, nitrate and sulfate ions could not be distinguished from the deposited PM, and they were extracted from all size of particles. Thus, the deposition velocities of both the ions were higher than those of PM_{10} and $PM_{2.5}$. The determined ion deposition velocity in this study was lower than that in studies using the gradient method (Takahashi and Wakamatsu, 2004) or knife-edge surrogate surfaces for particulate ion collection (Odabasi and Bagiroz, 2002; Shahin et al., 1999) but close to that in studies using deposition models (Luo et al., 2016; Morales et al., 1998; Zeller et al., 1997). Notably, the models in the aforementioned studies do not consider coarse particles ($d_p > 2.5$ μm) (Tasdemir and Günez, 2006); however, in our experiment, we considered ions of all particle sizes. The similar deposition velocities of nitrate and sulfate may suggest the existence of overestimation in these models. Therefore, additional field experiments must be conducted in the future to estimate the dry deposition velocities of PM and its associated soluble ions for ensuring the accuracy of dry deposition models applied in urban areas under different meteorological conditions.

4.4. Leaf particle loading effect

Understanding the limit of leaf particle loading is extremely important, and this parameter helps researchers to accurately estimate the amount of PM interception by urban forests over long periods of dry deposition. The amount of deposited PM particles increases under a high concentration and deposition velocity of PM but decreases due to PM resuspension (Wang et al., 2015); thus, PM deposition is a dynamic balancing process. Consequently, the PM retention capabilities of tree leaves may differ in different studies due to differences in tree species, PM ambient concentrations, and meteorological conditions. In this study, no visible decrease in TSP dry deposition distance was observed, which proved that no threshold of particle loading occurred during the dry deposition period (from 83 to 437 h) (Fig. 5). This finding agrees with those of previous studies, which have reported that the amount of dust retained by tree foliage increases with time for 20 days following a rain event (Qiu et al., 2009) and reaches a saturated state in 18–21 days (Zhou et al., 2020) or 24 days (Liu et al., 2012). Unfortunately, the dry deposition times of TSPs in our study were insufficiently long to determine the leaf loading threshold. Moreover, the deposition periods of PM_{10} and $PM_{2.5}$ were not widely distributed. The maximum TSP retention amount on leaves was observed at 437 h of dry deposition. The average TSP retention for all the species was 1.4 g m^{-2}, which is close to the result obtained by Liu et al. (2013), who determined a deposition saturation threshold of approximately 1.1 g m^{-2} for commercial or traffic areas.

Studies have indicated that less than 50% of PM is washed off by rainfall (Luo et al., 2019; Przybysz et al., 2014; Schaubroeck et al., 2014; Wang et al., 2006; Wang et al., 2015) and that rainfall duration and intensity affect the wash-off effect (Xu et al., 2017). In addition, $PM_{2.5}$ deposition is not necessarily washed off by rainfall (Xie et al., 2019). This phenomenon can be explained that small particles may be stuck due to the leaf microstructures. Thus, more residue of small particles on leaves after rainfall would appear than larger particles do (Wang et al., 2015). We divided the precipitation that occurred prior to dry deposition into different classes to examine the wash-off effect. No obvious increase of dry deposition distance was noted during low precipitation (black dot) in our study (Fig. 5), which indicated that a small amount of PM residue was left on the leaves or that the rainfall conditions did not affect the residue. The wash-off effect of PM from leaf surfaces after rainfall events significantly affected the initial dry deposition; thus, the residue of PM on leaves after rainfall overestimates the PM interception by trees. According to Xu et al. (2020), less than 10% of studies on leaf–PM interaction have focused on the wash-off effect. Therefore, future studies should conduct field experiments on the PM removal efficiency of rainfall to accurately calculate the total PM interception of urban forests.

4.5. Correlation analysis

By using Eq. (1), the dry deposition flux for leaves can be related to ambient concentration. This correlation is important for determining whether urban forests can retain a high PM interception ability during the air pollution season. However, (1) the applicability of the monitoring concentration; (2) the resuspension effect or residues on the leaf surface; and (3) other influencing factors, such as small-scale explosive events, lead to uncertainties in field experiments. In addition, if the deposition velocity remains unstable, the correlations can be weak (Mohan, 2016). Our results indicated that significant and positive correlations existed between the dry deposition flux and the ambient concentration for all the particles (Fig. 6), which suggests that urban forest can intercept PM on leaf surfaces when the air becomes polluted. Thus, hypothesis 3 is confirmed. The modest correlation between the aforementioned factors revealed that the deposition velocity was unstable over the sampling period. Fang et al. (2007) also found a low correlation between the aforementioned factors ($R^2 = 0.01$, 0.11, and 0.26 for fine, coarse, and TSPs, respectively) for the particles collected by PVC plates in Taichung.

The variation in the dry deposition velocity of PM can be attributed to the differences in meteorological conditions, particularly wind speed, which is a driving force that accelerates PM transport (Chen et al., 2012). A higher wind speed corresponds to a higher dry deposition velocity of small particles below a certain threshold. This result was obtained in wind tunnel experiments. The deposition velocity of $PM_{2.5}$ in i-Tree increases with wind speed for wind speeds below 10 m s^{-1} (Hirabayashi et al., 2015). Chen et al. (2016) indicated that the interception of $PM_{2.5}$ by trees is significantly correlated with wind speed ($r = 0.531$, $p < 0.01$); however, our results revealed that the deposition velocities of PM_{10} and $PM_{2.5}$ had a significant negative correlation with the wind speed (Table 1). This discrepancy was obtained probably because of the differences in the wind speed between the study of Chen et al. and the present study (the wind speed in the study of Chen et al. was below 6 m s^{-1}). In Taichung, the wind speed was low and stable during the sampling period (average values of 1.21 ± 0.28 m s^{-1} for TSPs monitoring period and 1.51 ± 0.24 m s^{-1} for PM_{10} and $PM_{2.5}$ monitoring period). Thus, strong correlations were not observed between wind speeds and PM deposition velocities in this study. In addition, the wind speed data from monitoring stations may not be applicable to areas near trees. A high wind speed not only brings particles from the emission source to nearby trees but also causes a strong resuspension effect. Moreover, the complex structure of trees can affect PM dispersion by reducing the wind speed or increasing the turbulence. Thus, the interaction among wind flows, trees, and particles can be highly complex. Consequently, the influence of meteorological conditions on PM dry deposition follows no universal law (Cai et al., 2017). Significant positive and modest correlations only occurred between relative humidity and small particles in this study. This phenomenon may be related to the hygroscopicity of particles, which enhances particle deposition (Hillamo et al., 1993).

5. Conclusion

This study, which analyzed results from field experiments, confirmed that the PM accumulation varied according to sampling time, site, and tree species. We selected five broadleaved tree species that are commonly found in Taiwan and have various leaf morphologies to examine the interception of PM and its associated ions. A significant relationship was observed between the ambient concentration and the dry deposition flux for all size fractions of PM. In addition, the temporal variations in the dry deposition of PM and its associated ions on different tree species exhibited similar trends, which suggests that tree leaves can be used as tools to monitor monthly air quality. The sulfate deposition on leaves indicated the possibility of the long-range transport of air pollutants. Overall, *K. elegans* exhibited higher $PM_{2.5}$ interception than *C. camphora* did, whereas *M. pinnata* exhibited the lowest TSP interception. Moreover, *B. javanica* was confirmed to intercept greater amounts of sulfate than the other species. This information is valuable when considering the air purification effect of planting trees. We determined that the dry deposition velocities of PM on leaf surfaces were 0.63, 0.062, and 0.028 cm s^{-1} for TSP, PM_{10}, and $PM_{2.5}$, respectively. Moreover, the dry deposition velocities of nitrate and sulfate were calculated to be 0.194 and 0.186 cm s^{-1}, respectively. The aforementioned parameters are valuable because they are established by weighing the dry deposition flux; thus, we can easily calculate the amount of PM or ion interception by urban forests directly through the concentration data obtained from monitoring stations in the future.

Three of the four research hypotheses were verified. However, the wind speed exhibited negative correlations with the PM deposition velocities, which contradicted the results from the wind tunnel experiments. Moreover, the dry deposition velocity of $PM_{2.5}$ in the i-Tree model was surprisingly very close to the field results, which suggests that we can accurately estimate the $PM_{2.5}$ removal by urban forests through the i-Tree model by using concentration monitoring data. However, the accuracy of estimating PM_{10} removal with the i-Tree model must still be confirmed. Further field studies should be conducted on the dry deposition flux and velocity of PM on leaves to ensure the accuracy of the i-Tree model. The threshold of leaf particle loading and the wash-off effect of rainfall or wind on PM should also be investigated in the future to avoid the overestimation of PM interception by urban forests.

Supplementary data to this article can be found online at https://doi.org/10.1016/j.scitotenv.2020.141788.

CRediT authorship contribution statement

Tzu-Hao Su: Conceptualization, Methodology, Investigation, Formal analysis, Writing - original draft. **Chin-Sheng Lin:** Investigation, Writing - review & editing. **Jiunn-Cheng Lin:** Writing - review & editing, Resources. **Chiung-Pin Liu:** Writing - review & editing, Supervision, Project administration.

Declaration of competing interest

The authors declare that they have no known competing financial interests or personal relationships that could have appeared to influence the work reported in this paper.

Acknowledgments

This research was financially supported by a grant (MOST 107-2313-B-005-009-) from the Ministry of Science Technology, Taiwan. We would also like to thank the i-Tree Cooperative for use of materials/graphics.

References

Armson, D., Rahman, M.A., Ennos, A.R., 2013. A comparison of the shading effectiveness of five different street tree species in Manchester, UK. Arboricult. Urban For. 39 (4), 157–164. https://doi.org/10.1007/s11252-014-0407-7.

Bandowe, B.A.M., Meusel, H., Huang, R.-J., Ho, K., Cao, J., Hoffmann, T., Wilcke, W., 2014. $PM_{2.5}$-bound oxygenated PAHs, nitro-PAHs and parent-PAHs from the atmosphere of a Chinese megacity: seasonal variation, sources and cancer risk assessment. Sci. Total Environ. 473-474, 77–87. https://doi.org/10.1016/j.scitotenv.2013.11.108.

Beckett, K., Freer-Smith, P., Taylor, G., 1998. Urban woodlands: their role in reducing the effects of particulate pollution. Environ. Pollut. 99 (3), 347–360. https://doi.org/10.1016/s0269-7491(98)00016-5.

Beckett, K.P., Freer-Smith, P.H., Taylor, G., 2000a. Particulate pollution capture by urban trees: effect of species and windspeed. Glob. Chang. Biol. 6 (8), 995–1003. https://doi.org/10.1046/j.1365-2486.2000.00376.x.

Beckett, K.P., Freer-Smith, P.H., Taylor, G., 2000b. Effective tree species for local air-quality management. J. Arboric. 26 (1), 12–19.

Bottalico, F., Chirici, G., Giannetti, F., Marco, A.D., Nocentini, S., Paoletti, E., ... Travaglini, D., 2016. Air Pollution Removal by Green Infrastructures and Urban Forests in the city of Florence. Agriculture and Agricultural Science Procedia 8, 243–251. https://doi.org/10.1016/j.aaspro.2016.02.099.

Cai, M., Xin, Z., Yu, X., 2017. Spatio-temporal variations in PM leaf deposition: a meta-analysis. Environ. Pollut. 231, 207–218. https://doi.org/10.1016/j.envpol.2017.07.105.

Chang, K.H., Jeng, F.T., Tsai, Y.L., Lin, P.L., 2000. Modeling of long-range transport on Taiwan's acid deposition under different weather conditions. Atmos. Environ. 34 (20), 3281–3295. https://doi.org/10.1016/s1352-2310(00)00072-8.

Chen, L., Peng, S., Liu, J., Hou, Q., 2012. Dry deposition velocity of total suspended particles and meteorological influence in four locations in Guangzhou, China. J. Environ. Sci. 24 (4), 632–639. https://doi.org/10.1016/s1001-0742(11)60805-x.

Chen, P., Bi, X., Zhang, J., Wu, J., Feng, Y., 2015a. Assessment of heavy metal pollution characteristics and human health risk of exposure to ambient $PM_{2.5}$ in Tianjin, China. Particuology 20, 104–109. https://doi.org/10.1016/j.partic.2014.04.020.

Chen, Y.C., Hsu, C.Y., Lin, S.L., Chang-Chien, G.P., Chen, M.J., Fang, G.C., Chiang, H.C., 2015b. Characteristics of concentrations and metal compositions for $PM_{2.5}$ and $PM_{2.5–10}$ in Yunlin County, Taiwan during air quality deterioration. Aerosol Air Qual. Res. 15 (7), 2571–2583. https://doi.org/10.4209/aaqr.2015.04.0261.

Chen, L., Liu, C., Zou, R., Yang, M., Zhang, Z., 2016. Experimental examination of effectiveness of vegetation as bio-filter of particulate matters in the urban environment. Environ. Pollut. 208, 198–208. https://doi.org/10.1016/j.envpol.2015.09.006.

Chen, L., Liu, C., Zhang, L., Zou, R., Zhang, Z., 2017. Variation in tree species ability to capture and retain airborne fine particulate matter ($PM_{2.5}$). Sci. Rep. 7 (1). https://doi.org/10.1038/s41598-017-03360-1.

Dzierżanowski, K., Popek, R., Gawrońska, H., Sæbø, A., Gawroński, S.W., 2011. Deposition of particulate matter of different size fractions on leaf surfaces and in waxes of urban forest species. International Journal of Phytoremediation 13 (10), 1037–1046. https://doi.org/10.1080/15226514.2011.552929.

Fang, G.C., Chang, C.N., Chu, C.C., Wu, Y.S., Fu, P.P.C., Yang, I.L., Chen, M.H., 2003. Characterization of particulate, metallic elements of TSP, $PM_{2.5}$ and $PM_{2.5-10}$ aerosols at a farm sampling site in Taiwan, Taichung. Sci. Total Environ. 308 (1–3), 157–166. https://doi.org/10.1016/S0048-9697(02)00648-4.

Fang, G.-C., Wu, Y.-S., Lee, W.-J., Chou, T.-Y., Lin, I.-C., 2007. Ambient air particulates, metallic elements, dry deposition and concentrations at Taichung Airport, Taiwan. Atmos. Res. 84 (3), 280–289. https://doi.org/10.1016/j.atmosres.2006.08.006.

Freer-Smith, P., Holloway, S., Goodman, A., 1997. The uptake of particulates by an urban woodland: site description and particulate composition. Environ. Pollut. 95 (1), 27–35. https://doi.org/10.1016/s0269-7491(96)00119-4.

Gonzalez-Sosa, E., Braud, I., Piña, R.B., Loza, C.A.M., Salinas, N.M.R., Chavez, C.V., 2017. A methodology to quantify ecohydrological services of street trees. Ecohydrology & Hydrobiology 17 (3), 190–206. https://doi.org/10.1016/j.ecohyd.2017.06.004.

Han, L., Zhuang, G., Cheng, S., Wang, Y., Li, J., 2007. Characteristics of re-suspended road dust and its impact on the atmospheric environment in Beijing. Atmos. Environ. 41 (35), 7485–7499. https://doi.org/10.1016/j.atmosenv.2007.05.044.

Hillamo, R.E., Kerminen, V.M., Maenhaut, W., Jaffrezo, J.L., Balachandran, S., Davidson, C.I., 1993. Size distributions of atmospheric trace elements at dye 3, Greenland — I. distribution characteristics and dry deposition velocities. Atmos. Environ. Part A 27 (17–18), 2787–2802. https://doi.org/10.1016/0960-1686(93)90311-l.

Hirabayashi, S., Kroll, C.N., Nowak, D.J., 2015. i-Tree eco dry deposition model descriptions. Retrieved from. https://www.itreetools.org/eco/resources/iTree_Eco_Dry_Deposition_Model_Descriptions.pdf.

Ho, K.F., Lee, S.C., Chan, C.K., Yu, J.C., Chow, J.C., Yao, X.H., 2003. Characterization of chemical species in $PM_{2.5}$ and PM_{10} aerosols in Hong Kong. Atmos. Environ. 37, 31–39. https://doi.org/10.1016/S1352-2310(02)00804-X.

Hofman, J., Wuyts, K., Wittenberghe, S.V., Brackx, M., Samson, R., 2014. On the link between biomagnetic monitoring and leaf-deposited dust load of urban trees: relationships and spatial variability of different particle size fractions. Environ. Pollut. 192, 285–294. https://doi.org/10.1016/j.envpol.2014.05.006.

Horváth, L., 2003. Dry deposition velocity of $PM_{2.5}$ ammonium sulfate particles to a Norway spruce forest on the basis of S- and N-balance estimations. Atmos. Environ. 37 (31), 4419–4424. https://doi.org/10.1016/s1352-2310(03)00584-3.

Hsu, C.Y., Chiang, H.C., Lin, S.L., Chen, M.J., Lin, T.Y., Chen, Y.C., 2016. Elemental characterization and source apportionment of PM_{10} and $PM_{2.5}$ in the western coastal area of central Taiwan. Sci. Total Environ. 541, 1139–1150. https://doi.org/10.1016/j.scitotenv.2015.09.122.

Kong, S., Yan, Q., Zheng, H., Liu, H., Wang, W., Zheng, S., Huang, M., 2018. Substantial reductions in ambient PAHs pollution and lives saved as a co-benefit of effective long-term $PM_{2.5}$ pollution controls. Environ. Int. 114, 266–279. https://doi.org/10.1016/j.envint.2018.03.002.

Leonard, R.J., Mcarthur, C., Hochuli, D.F., 2016. Particulate matter deposition on roadside plants and the importance of leaf trait combinations. Urban For. Urban Green. 20, 249–253. https://doi.org/10.1016/j.ufug.2016.09.008.

Li, Z., Ma, Z., Kuijp, T.J.V.D., Yuan, Z., Huang, L., 2014. A review of soil heavy metal pollution from mines in China: pollution and health risk assessment. Sci. Total Environ. 468-469, 843–853. https://doi.org/10.1016/j.scitotenv.2013.08.090.

Lin, C.Y., Wang, Z., Chen, W.N., Chang, S.Y., Chou, C.C.K., Sugimoto, N., Zhao, X., 2007. Long-range transport of Asian dust and air pollutants to Taiwan: observed evidence and model simulation. Atmospheric Chemistry and Physics Discussions 7, 423–434. https://doi.org/10.5194/acpd-6-10183-2006.

Litschke, T., Kuttler, W., 2008. On the reduction of urban particle concentration by vegetation a review. Meteorol. Z. 17 (3), 229–240. https://doi.org/10.1127/0941-2948/2008/0284.

Liu, L., Guan, D., Peart, M.R., 2012. The morphological structure of leaves and the dust-retaining capability of afforested plants in urban Guangzhou, South China. Environ. Sci. Pollut. Res. 19 (8), 3440–3449. https://doi.org/10.1007/s11356-012-0876-2.

Liu, L., Guan, D., Peart, M.R., Wang, G., Zhang, H., Li, Z., 2013. The dust retention capacities of urban vegetation—a case study of Guangzhou, South China. Environ. Sci. Pollut. Res. 20 (9), 6601–6610. https://doi.org/10.1007/s11356-013-1648-3.

Long, C.M., Suh, H.H., Catalano, P.J., Koutrakis, P., 2001. Using time- and size-resolved particulate data to quantify indoor penetration and deposition behavior. Environmental Science & Technology 35 (10), 2089–2099. https://doi.org/10.1021/es011283d.

Lovett, G.M., 1994. Atmospheric deposition of nutrients and pollutants in North America: an ecological perspective. Ecol. Appl. 4 (4), 629–650. https://doi.org/10.2307/1941997.

Luo, X., Pan, Y., Goulding, K., Zhang, L., Liu, X., Zhang, F., 2016. Spatial and seasonal variations of atmospheric sulfur concentrations and dry deposition at 16 rural and suburban sites in China. Atmos. Environ. 146, 79–89. https://doi.org/10.1016/j.atmosenv.2016.07.038.

Luo, J., Niu, Y., Zhang, Y., Zhang, M., Tian, Y., Zhou, X., 2019. Dynamic analysis of retention $PM_{2.5}$ by plant leaves in rainfall weather conditions of six tree species. Energy Sources, Part A: Recovery, Utilization, and Environmental Effects 42 (8), 1014–1025. https://doi.org/10.1080/15567036.2019.1602212.

Ma, Q., Cai, S., Wang, S., Zhao, B., Martin, R.V., Brauer, M., Burnett, R.T., 2017. Impacts of coal burning on ambient PM2.5 pollution in China. Atmos. Chem. Phys. 17 (7), 4477–4491. https://doi.org/10.5194/acp-2016-601.

Mohammed, M.O., Song, W.W., Ma, Y.L., Liu, L.Y., Ma, W.L., Li, W.L., Khan, A.U., 2016. Distribution patterns, infiltration and health risk assessment of $PM_{2.5}$-bound PAHs in indoor and outdoor air in cold zone. Chemosphere 155, 70–85. https://doi.org/10.1016/j.chemosphere.2016.04.023.

Mohan, S.M., 2016. An overview of particulate dry deposition: measuring methods, deposition velocity and controlling factors. Int. J. Environ. Sci. Technol. 13 (1), 387–402. https://doi.org/10.1007/s13762-015-0898-7.

Morales, J.A., Bifano, C., Escalona, A., 1998. Atmospheric deposition of SO_4–S and (NH_4+NO_3)–N at two rural sites in the Western Maracaibo Lake Basin, Venezuela. Atmos. Environ. 32 (17), 3051–3058. https://doi.org/10.1016/s1352-2310(97)00160-x.

Mori, J., Hanslin, H.M., Burchi, G., Sæbø, A., 2015. Particulate matter and element accumulation on coniferous trees at different distances from a highway. Urban For. Urban Green. 14 (1), 170–177. https://doi.org/10.1016/j.ufug.2014.09.005.

Nowak, D.J., Hirabayashi, S., Bodine, A., Hoehn, R., 2013. Modeled $PM_{2.5}$ removal by trees in ten U.S. cities and associated health effects. Environ. Pollut. 178, 395–402. https://doi.org/10.1016/j.envpol.2013.03.050.

Odabasi, M., Bagiroz, H.O., 2002. Sulfate dry deposition fluxes and overall deposition velocities measured with a surrogate surface. Sci. Total Environ. 297 (1–3), 193–201. https://doi.org/10.1016/s0048-9697(02)00127-4.

Popek, R., Gawrońska, H., Wrochna, M., Gawroński, S.W., Sæbø, A., 2013. Particulate matter on foliage of 13 woody species: deposition on surfaces and phytostabilisation in waxes – a 3-year study. International Journal of Phytoremediation 15 (3), 245–256. https://doi.org/10.1080/15226514.2012.694498.

Prajapati, S.K., Tripathi, B.D., 2008. Seasonal variation of leaf dust accumulation and pigment content in plant species exposed to urban particulates pollution. Journal of Environmental Quality 37 (3), 865. https://doi.org/10.2134/jeq2006.0511.

Prusty, B., Mishra, P., Azeez, P., 2005. Dust accumulation and leaf pigment content in vegetation near the national highway at Sambalpur, Orissa, India. Ecotoxicol. Environ. Saf. 60 (2), 228–235. https://doi.org/10.1016/j.ecoenv.2003.12.013.

Przybysz, A., Sæbø, A., Hanslin, H.M., Gawroński, S.W., 2014. Accumulation of particulate matter and trace elements on vegetation as affected by pollution level, rainfall and the passage of time. Sci. Total Environ. 481, 360–369. https://doi.org/10.1016/j.scitotenv.2014.02.072.

Qiu, Y., Guan, D., Song, W., Huang, K., 2009. Capture of heavy metals and sulfur by foliar dust in urban Huizhou, Guangdong Province, China. Chemosphere 75 (4), 447–452. https://doi.org/10.1016/j.chemosphere.2008.12.061.

Sæbø, A., Popek, R., Nawrot, B., Hanslin, H., Gawronska, H., Gawronski, S., 2012. Plant species differences in particulate matter accumulation on leaf surfaces. Sci. Total Environ. 427-428, 347–354. https://doi.org/10.1016/j.scitotenv.2012.03.084.

Schaubroeck, T., Deckmyn, G., Neirynck, J., Staelens, J., Adriaenssens, S., Dewulf, J., Verheyen, K., 2014. Multilayered modeling of particulate matter removal by a growing forest over time, from plant surface deposition to Washoff via rainfall. Environmental Science & Technology 48 (18), 10785–10794. https://doi.org/10.1021/es5019724.

Selmi, W., Weber, C., Rivière, E., Blond, N., Mehdi, L., Nowak, D., 2016. Air pollution removal by trees in public green spaces in Strasbourg city, France. Urban For. Urban Green. 17, 192–201. https://doi.org/10.1016/j.ufug.2016.04.010.

Sgrigna, G., Sæbø, A., Gawronski, S., Popek, R., Calfapietra, C., 2015. Particulate matter deposition on *Quercus ilex* leaves in an industrial city of Central Italy. Environ. Pollut. 197, 187–194. https://doi.org/10.1016/j.envpol.2014.11.030.

Shahin, U.M., Zhu, X., Holsen, T.M., 1999. Dry deposition of reduced and reactive nitrogen: a surrogate surfaces approach. Environmental Science & Technology 33 (12), 2113–2117. https://doi.org/10.1021/es981299c.

Song, Y., Maher, B.A., Li, F., Wang, X., Sun, X., Zhang, H., 2015. Particulate matter deposited on leaf of five evergreen species in Beijing, China: source identification and size distribution. Atmos. Environ. 105, 53–60. https://doi.org/10.1016/j.atmosenv.2015.01.032.

Sosa, B.S., Porta, A., Lerner, J.E.C., Noriega, R.B., Massolo, L., 2017. Human health risk due to variations in PM 10 -PM 2.5 and associated PAHs levels. Atmos. Environ. 160, 27–35. https://doi.org/10.1016/j.atmosenv.2017.04.004.

Takahashi, A., Wakamatsu, T., 2004. Estimation of deposition velocity of particles to a forest using the concentration gradient method. Journal of Japan Society for Atmospheric Environment 39, 53–61 (in Japanese).

Tallis, M., Taylor, G., Sinnett, D., Freer-Smith, P., 2011. Estimating the removal of atmospheric particulate pollution by the urban tree canopy of London, under current and future environments. Landsc. Urban Plan. 103 (2), 129–138. https://doi.org/10.1016/j.landurbplan.2011.07.003.

Tasdemir, Y., Günez, H., 2006. Ambient concentration, dry deposition flux and overall deposition velocities of particulate sulfate measured at two sites. Atmos. Res. 81 (3), 250–264. https://doi.org/10.1016/j.atmosres.2006.01.002.

Tsai, J.H., Lin, J.H., Yao, Y.C., Chiang, H.L., 2012. Size distribution and water soluble ions of ambient particulate matter on episode and non-episode days in southern Taiwan. Aerosol Air Qual. Res. 12 (2), 263–274. https://doi.org/10.4209/aaqr.2011.10.0167.

Wang, L., Liu, L.Y., Gao, S.Y., Hasi, E., Wang, Z., 2006. Physicochemical characteristics of ambient particles settling upon leaf surfaces of urban plants in Beijing. J. Environ. Sci. 18 (5), 921–926. https://doi.org/10.1016/s1001-0742(06)60015-6.

Wang, J., Endreny, T.A., Nowak, D.J., 2008. Mechanistic simulation of urban tree effects in an urban water balance model. Journal of American Water Resource Association 44 (1), 75–85.

Wang, H., Shi, H., Li, Y., Yu, Y., Zhang, J., 2013. Seasonal variations in leaf capturing of particulate matter, surface wettability and micromorphology in urban tree species. Frontiers of Environmental Science & Engineering 7 (4), 579–588. https://doi.org/10.1007/s11783-013-0524-1.

Wang, H., Shi, H., Wang, Y., 2015. Effects of weather, time, and pollution level on the amount of particulate matter deposited on leaves of *Ligustrum lucidum*. Sci. World J. 2015, 1–8. https://doi.org/10.1155/2015/935942.

Wang, F., Zhou, Y., Meng, D., Han, M., Jia, C., 2018. Heavy metal characteristics and health risk assessment of $PM_{2.5}$ in three residential homes during winter in Nanjing, China. Build. Environ. 143, 339–348. https://doi.org/10.1016/j.buildenv.2018.07.011.

Weerakkody, U., Dover, J.W., Mitchell, P., Reiling, K., 2018. Quantification of the traffic-generated particulate matter capture by plant species in a living wall and evaluation of the important leaf characteristics. Sci. Total Environ. 635, 1012–1024. https://doi.org/10.1016/j.scitotenv.2018.04.106.

Xie, Y., Zhao, B., Zhao, Y., Luo, Q., Wang, S., Zhao, B., Bai, S., 2017. Reduction in population exposure to PM 2.5 and cancer risk due to $PM_{2.5}$-bound PAHs exposure in Beijing, China during the APEC meeting. Environ. Pollut. 225, 338–345. https://doi.org/10.1016/j.envpol.2017.02.059.

Xie, C., Yan, L., Liang, A., Che, S., 2019. Understanding the washoff processes of $PM_{2.5}$ from leaf surfaces during rainfall events. Atmos. Environ. 214, 116844. https://doi.org/10.1016/j.atmosenv.2019.116844.

Xu, X., Zhang, Z., Bao, L., Mo, L., Yu, X., Fan, D., Lun, X., 2017. Influence of rainfall duration and intensity on particulate matter removal from plant leaves. Sci. Total Environ. 609, 11–16. https://doi.org/10.1016/j.scitotenv.2017.07.141.

Xu, Y., Xu, W., Mo, L., Heal, M.R., Xu, X., Yu, X., 2018. Quantifying particulate matter accumulated on leaves by 17 species of urban trees in Beijing, China. Environ. Sci. Pollut. Res. 25 (13), 12545–12556. https://doi.org/10.1007/s11356-018-1478-4.

Xu, X., Xia, J., Gao, Y., Zheng, W., 2020. Additional focus on particulate matter wash-off events from leaves is required: a review of studies of urban plants used to reduce airborne particulate matter pollution. Urban For. Urban Green. 48, 126559. https://doi.org/10.1016/j.ufug.2019.126559.

Yang, K.L., 2002. Spatial and seasonal variation of PM_{10} mass concentrations in Taiwan. Atmos. Environ. 36 (21), 3403–3411. https://doi.org/10.1016/s1352-2310(02)00312-6.

Zeller, K., Donev, E., Bojinov, H., Nikolov, N., 1997. Air pollution status of the Bulgarian Govedartsi ecosystem. Environ. Pollut. 98 (3), 281–289. https://doi.org/10.1016/s0269-7491(97)00144-9.

Zheng, X., Xu, X., Yekeen, T.A., Zhang, Y., Chen, A., Kim, S.S., Huo, X., 2016. Ambient air heavy metals in $PM_{2.5}$ and potential human health risk assessment in an informal electronic-waste recycling site of China. Aerosol Air Qual. Res. 16 (2), 388–397. https://doi.org/10.4209/aaqr.2014.11.0292.

Zhou, M., Wang, X., Lin, X., Yang, S., Zhang, J., Chen, J., 2020. Automobile exhaust particles retention capacity assessment of two common garden plants in different seasons in the Yangtze River Delta using open-top chambers. Environ. Pollut. 263, 114560. https://doi.org/10.1016/j.envpol.2020.114560.